

# EFFECT OF ATMOSPHERIC TURBULENCE ON A LAMINAR BOUNDARY-LAYER.

Fabio P. Bertolotti

*Presented at the XXVI OSTIV Congress, Bayreuth, Germany*

## SUMMARY

In connection with the loss of glide performance experienced by some sailplanes upon entering the turbulent air in thermals, we review experimental and theoretical investigations into the response of a laminar boundary layer to external (e.g. atmospheric) turbulence. Contrary to intuition, the excitation of Tollmien-Schlichting waves is such a feeble process that it is unlikely to play any significant role at all. The excitation of low frequency, high amplitude streaks, on the other hand, is a very efficient process that must be considered as a likely source of early laminar-turbulent transition within the boundary-layer.

## 1 INTRODUCTION

In a personal communication, Waibel<sup>1</sup> reports that pilots of sailplanes have experienced a loss of glide performance after entering the turbulent air found in thermals. Measurements of the spectrum of the atmospheric turbulence show that most of the energy is contained at frequencies much lower than those of the unstable TS waves in the airfoil's boundary layer. Nevertheless, Waibel, and others, suspect that the loss of performance comes from a premature transition to turbulent flow over the wings' surface. Some insight into this phenomenon can be gained from the basic experimental and theoretical studies made in the past decades on a simpler geometry, namely a flat-plate at zero angle of attack. These studies have spanned the multitude of ways traveling waves and other disturbances within the laminar boundary-layer are generated by an external forcing, including free-stream turbulence, sound, surface roughness, and surface suction. This topic has received the name "receptivity" in the technical literature. Herein, we briefly review the main receptivity processes relevant to sailplane conditions, and show that the low-frequency components of turbulence impinging on the wing cause the largest response in the boundary-layer, and are, thus, likely culprits for the loss of performance in thermals. We then expose a theoretical model for the underlying receptivity process.

Essentially two types of receptivity processes are active on a sailplane wing: those that scatter free-stream turbulence and sound and excite traveling waves (Tollmien-Schlichting waves) having a frequency of hundreds of Hertz, and those that directly couple free-stream turbulence to the boundary-layer response and excite motions at a few Hertz. This division follows the two types of boundary-layer instabilities given by the well known Orr-Sommerfeld equation: traveling waves, which appear as discrete modes in the spectrum of solutions, and

convected motions, which appear as modes of the continuous part of the spectrum.

Traveling waves (TS waves) propagate downstream at a velocity that is roughly one third the free-stream velocity<sup>2</sup>. Since the turbulence in the free-stream travels with the free-stream, hence faster, the turbulence cannot directly couple to, and feed energy to, the TS waves. An even greater mismatch in propagation velocity occurs between TS waves and sound in the free-stream. A match in velocity and transfer of energy can occur, however, when the free-stream turbulence and sound waves are scattered at the surface of the wing by small roughness. The interaction between the free-stream turbulence and the wall roughness creates a disturbance in the boundary-layer that has the same speed as the TS wave, and can, thus, feed energy into the TS wave. In contrast, the other type of receptivity process occurs at low frequencies and is characterized by a direct coupling between the boundary-layer response and the free-stream turbulence. Since scattering is not needed, this process occurs even over wing surfaces that are perfectly smooth. The response takes the form of thickening and thinning of the displacement thickness, and was described by Klebanoff and Tidstrom [1] as a "breathing mode" after being first measured in wind-tunnel experiments in the late 50's. Another, more modern, description is "streaks." The coupling is most efficient in the limit of zero frequency, and can lead to velocity deviations in the boundary-layer as large as 10% of the free-stream velocity (TS waves reach 1 to 2% at transition). Although these streaks alone can lead the flow into turbulence when the streaks reach sufficiently high amplitudes to create localized and intense shear layers, they can also accelerate the transition process at lower amplitudes when a weak TS wave is present.

Before focusing on the low-frequency response, I would like to offer three reasons why I believe the scattering process of turbulence is a weak process on sailplane wings. First, the turbulence components at the frequency of TS waves, typically several hundred Hertz, have small energies. Second, the surface of wings is usually polished and free of the roughness necessary for scatter. Third, at TS wave frequencies, the free-stream turbulence does not penetrate well into the boundary-layer. Figure 1-a, taken from [2], shows how inefficiently modes of free-stream turbulence at TS-wave frequencies penetrate into the boundary layer. Near the wall, where the scattering process takes place, the velocity magnitude is quite small. Thus, even on an un-polished wing with roughness at the wall, the scattering is weak. This last argument fails for acoustic waves, which penetrate the boundary-layer to the wall (see figure 1-b), creating a Stokes layer there. But the acoustic field in thermals is weak, and no more intense than elsewhere, so also the forcing from acoustic scatter remains weak. Lastly, scattering can also occur on regions of the airfoil with large curvature, e.g. at the leading edge. This particular form of turbulence scattering has not been studied in detail, and could be important on swept wings since there the neutral stability point for cross-flow instabilities

lies close to the attachment line. Sailplane wings have negligible sweep, and the neutral stability point for TS waves lies far from the leading edge, typically near the peak-suction location at 25% to 35% chord, so also this form of scattering is weak on the unswept wings of sail planes.

As we will show in the remainder of this paper, forcing from the low-frequency components of atmospheric turbulence is quite effective in creating disturbances in the wing's boundary-layer. Indeed, these disturbances are

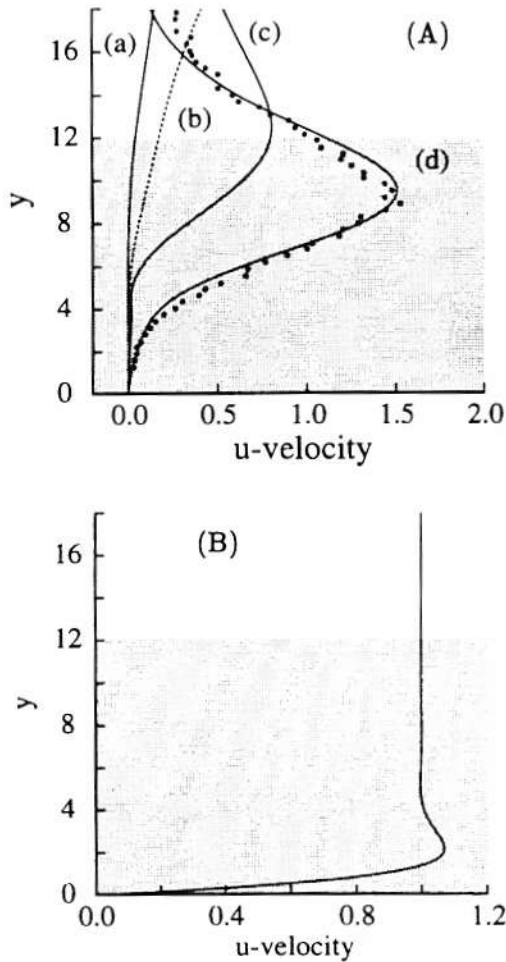


Figure 1: Streamwise velocity (arbitrary scale) versus wall-normal distance. (A) Penetration of high-frequency turbulence into the boundary-layer (gray region). Cases (a) and (b) for vortical modes of "A" type; (c) and (d) for "B" type (see ref [2] and section 3). Non-dimensional frequency  $F = 60$ , where  $F = 2\pi f v \times 10^6 / U^2 \propto$ , and  $f$  in Hertz. Symbols from experiments [3]. (B) Penetration of an acoustic wave, also at  $F = 60$ .

much larger in amplitude than the freestream turbulence itself, with the amplification factor scaling with the square-root of the local Reynolds number and reaching values of 50 or more. Consequently, eddies in the atmospheric turbulence with velocities smaller than 0.1% of the sailplane's velocity can still lead to large disturbances in the wing's boundary-layer. We limit our discussion to the flat-plate geometry at zero angle of attack, rather than a true airfoil, but the physics of the receptivity process remain equally valid for a sailplane wing.

The contents of this paper are organized as follows. In section 2 we present an overview of experimental findings. In sections 3.1 and 3.2 we present the main steps in a theoretical and numerical model developed by the author and compare and discuss results with experimental data. In section 3.3 we present the results from an improved comparison between theory and experiment aimed at removing uncertainties in the experimental measurement of the turbulent length-scales.

## 2 THE EXPERIMENTS

The first observation of streaks in two-dimensional boundary-layers came in the late 50's when Klebanoff and co-workers [4] measured an anomalous boundary-layer velocity field containing a spanwise modulation of the streamwise velocity. After some investigations, they were able to trace the source to the turbulence produced by the wind-tunnel screens. Figure 2 portrays, with some artistic freedom, the essential features of the boundary-layer response. The undulating surface denotes the edge of the boundary-layer, which undergoes a spanwise modulation with wavelength  $\lambda_z$ . The deviation of streamwise velocity from the undisturbed state is also shown at two spanwise locations. When the deviation is aligned with the basic velocity field, the thickness of the boundary-layer decreases, and vice-versa when the velocity is aligned contrary to the basic velocity field. The velocity deviation, alias the response produced within the layer, is today referred to as the Klebanoff mode (K-mode in short, but not to be confused with "Klebanoff-type" secondary instability) or, alternatively, as streaks. The K-mode can oscillate slowly in time and since the receptivity process is linear, as discussed below in the theoretical model, many K-modes can occur simultaneously, each having a specific wavelength  $\lambda_z$  and frequency  $\omega$ . In later experiments, Kendall [3] [5] produced free-stream turbulence of

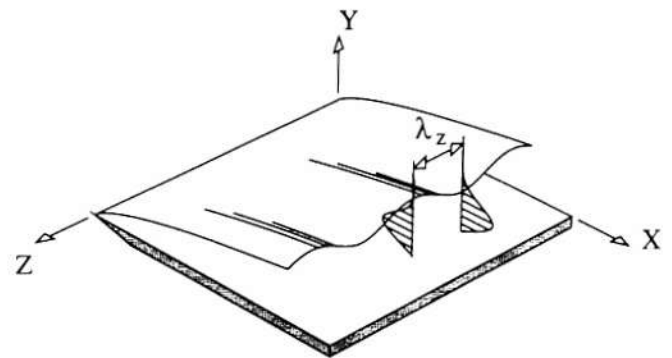


Figure 2: Spanwise variation of the boundary-layer thickness associated with a Klebanoff mode (alias "streak"), and streamwise velocity deviation from the Blasius profile at maximum and minimum of the thickness.

adjustable level in the wind-tunnel and observed an approximately linear dependence between the turbulence level and the amplitude of the resultant Klebanoff-mode boundary layer fluctuations on a flat plate test model. Other characteristics observed were that the amplitude of

the broad-band (in frequency) fluctuations grew with the square-root of the streamwise coordinate, that the lateral correlation scale was commensurate with that of the free-stream turbulence, and that the temporal frequencies were far lower than those of T-S waves which would be unstable. His observations have been experimentally confirmed by Westin et al. [6]. Kendall also saw no change in the boundary-layer response when the leading-edge geometry was changed. Earlier measurements of Kachanov, Kozlov and Levchenko [7] [8] of the vortical field generated by a vibrating ribbon positioned upstream of a non-swept plate also showed weak amplification due to vortex stretching and tilting at the leading edge.

### 3 THEORY

Theoretical models provide significant help in understanding the receptivity process. For example, the reviews by Goldstein & Hultgreen [9] and Kerschen [10] of asymptotic methods, Crouch [11] and Choudhari & Street [12] of classical finite Reynolds-Number models, and Hill [13] of the adjoint model, provide an overview of the scattering process. In contrast, much less work has been published on the analysis of the low-frequency process. Herein, we follow the model for the low-frequency process presented in [2] since this model exposes, in the author's opinion, the main ingredients of the physics involved. The blueprint for the model can be constructed by consideration of the experimental observations. In particular, four observations are pivotal: a) the response scales linearly with the forcing, b) the spanwise scale inside and outside the boundary-layer are commensurate, c) the growth of the broad-band frequency response is proportional to  $\sqrt{x}$ , and d) the leading-edge geometry has little influence on low-frequency motions in the flow over a flat plate with no sweep angle.

The  $\sqrt{x}$  growth suggests that the response is governed by equations of the boundary layer type. The linear response and the match in spanwise length-scale suggest that the atmospheric turbulence appears directly as a forcing in these equations. Lastly, the insensitivity to the leading-edge geometry suggests that the leading-edge region has a negligible effect on the low-frequency turbulence, so the singular nature of the boundary-layer equations at the leading-edge must not be dealt with. Additional motives for a linear model based on the boundary-layer equations comes from Crow's [14] asymptotic analysis of the Klebanoff mode, made in the mid 1960's.

The receptivity model, thus, comprises three steps. First, a decomposition of the atmospheric turbulence into vortical modes is made (Fourier decomposition). Then, the response of the boundary-layer (streaks) to each mode is investigated using the linearized Prandtl boundary-layer equations (in our case, we use the Parabolized Stability Equations [15] that contain Prandtl's equations in the limit of zero frequency), and the atmospheric modes that generated the largest response are identified. This step includes studying the effect of frequency and spatial scales. Lastly, the full non-linear stability equations are solved for the

evolution of streaks and traveling waves and the location of skin-friction rise as function of turbulence strength is studied.

#### 3.1 THE FREE-STREAM MODES

The turbulence in a wind-tunnel is generated by screens upstream of the test-section, and has (root-mean-square) velocity fluctuations in the order of one percent (or less) of the mean velocity. After generation, the turbulence is essentially convected downstream without exchange of energy between the turbulent scales, since the Reynolds stresses, which scale with the square of the fluctuation velocity, are negligible at these fluctuation strengths. The convected turbulent field, thus, can be represented as a summation of modes that solve the Navier-Stokes equations linearized about a steady flow with constant streamwise velocity. These modes are easy to calculate, and can be partitioned into two families that I call the "A" and "B" type. A mathematical expression for these modes is given in [2], and consists essentially of sinusoidal variation in all three space directions and time,

$$\mathbf{v}(x, y, z, t) = \mathbf{v}_0 \cos(\omega(x/U_\infty - t) + \beta z + \delta y) \quad (1)$$

where  $\mathbf{v}_0$  is constant,  $U_\infty$  is the velocity in the free-stream,  $x$  is aligned in the streamwise direction,  $z$  in the spanwise direction, and  $y$  normal to the wall. These modes are the

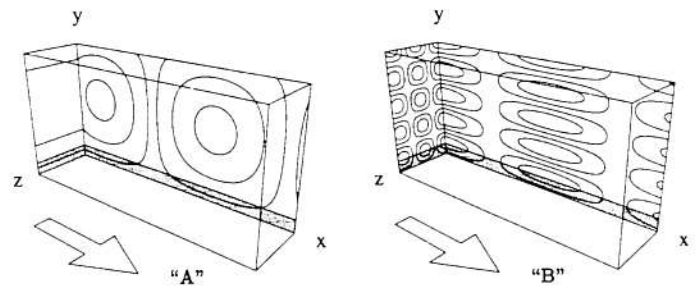


Figure 3: Iso-contours of the magnitude of vorticity for free-stream modes of type "A" and "B". The nondimensional frequency is  $F = 56$ . The arrow indicates the free-stream direction, and the gray-bands indicate the region the boundary-layer would occupy if a flat plate was present.

vortical modes discussed in the context of compressible flow by Chu and Kovasznay in the late 50's [16]. Figure 3 displays the nature of the two families. Type "A" modes are structures aligned perpendicular to the flow direction, whose size in the  $x - y$  plane scales as  $U_\infty/\omega$ . Thus, type "A" modes necessarily have a non-zero frequency (imagine the signal from a fixed hot-wire in the free-stream as the structure passes by). The modes of type "B", on the other hand, have structures aligned with the flow. The mode shown in figure 3 has a non-zero frequency, as evident from the periodic variation in the stream direction. In the limit of zero frequency, the streamwise variation vanishes, leaving steady stream-wise aligned vortices, with scales  $\lambda_z = 2\pi/\beta$  and  $\lambda_y = 2\pi/\delta$  in the plane normal to the flow. In the figure,  $\beta = \delta$  so the iso-contours are circles in

the  $y$ - $z$  plane, but other combinations of  $\beta$  and  $\delta$  lead to elliptical cross-sections. The values of  $\beta$  and  $\delta$  are fixed for each mode, and the variation of  $\beta$  and  $\delta$  over a continuous range of values creates a family of modes. The actual turbulent flow field is composed of a superposition of many these "A" and "B" of modes. Indeed, any vortical field can be constructed from the linear superposition of these modes, and we take advantage of this fact in section 3.3 to improve comparison between theory and experiment.

I expect the above results for turbulent flow in a wind-tunnel's test-section to carry over to the atmospheric turbulence about a sailplane wing. The speed of the sail plane is significantly higher than that of the turbulence in a thermal. An observer fixed on the wing would see the atmospheric turbulence as vortical modes convected in the flow about the wing. The relevant low-frequency components would appear as "long vortical tubes" aligned with the flow streamlines.

### 3.2 THE BOUNDARY-LAYER RESPONSE

The equations governing the boundary-layer response will not be given here for reasons of space, but the equations are presented and discussed in depth in [2]. As first step, a mode of type "B" with arbitrary scales  $\beta$  and  $\delta$  is selectively introduced in a otherwise laminar and undisturbed free-stream. As amplitude we can choose unity, since the problem is linear. Figure 4 displays the two-step solution procedure used to evaluate the boundary-layer response. The first step comprises a rapidly convergent series solution to the unsteady boundary layer equation

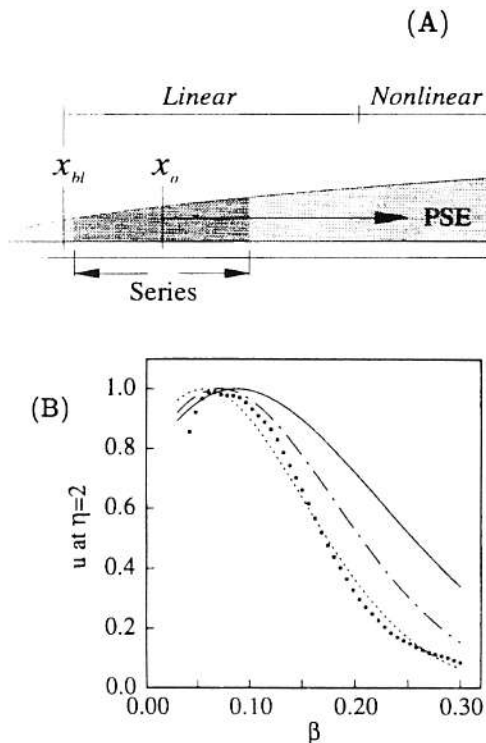


Figure 4: (A) Illustration of the two-step solution procedure (B) Streak amplitude, based on maximum streamwise velocity, as function of spanwise wave number  $\beta$  at  $Rx = 720$ . Symbols derived from Kendall's experiment [3]. Solid lines from theory [2], using different assumptions of the anisotropic state of the free-stream turbulence.

in which the "B" mode appears as forcing. The series converges over a region that excludes the vicinity of the leading edge and extends downstream to the point  $x_n$  where the parabolized stability equations (PSE) [15] [17] [18] can be started. The PSE include the unsteady boundary-layer equations, but have the added advantage of also modeling Tollmien-Schlichting waves and the non-linear mode interaction that necessarily precedes the onset of turbulence inside the boundary-layer. Herein, the results in figure 6 are from a non-linear calculation - all other results are from solutions to the linearized equations. In all cases, the PSE incorporate the forcing from the "B" mode at low frequencies, and within the region denoted "linear" in figure 4-a the response scales linearly with the strength of the free-stream mode.

The procedure is repeated for a wide variety of  $\beta$  and  $\delta$  values (i.e. scales), and the total response is obtained as the linear superposition of solutions with weights correspondent to the energies of the "B" mode in the atmospheric turbulence. Ideally, an experimental measurement would provide us with the energies at all length-scales in actual flight, but such a measurement is hopelessly beyond our current measurement abilities. Thus, we proceed with an alternative strategy, and search for the values of the parameters  $\beta$  and  $\delta$  that lead to the largest boundary-layer response. The result of scanning values of  $\beta$  and  $\delta$  is shows a clear maximum at specific values of  $\beta$  and  $\delta$  and zero frequency. The spanwise scale is roughly 8 to 10 times the boundary-layer thickness (99% definition) and the wall normal scale (i.e.  $\delta$ ) is slightly larger. In the following discussion we refer to the "B" mode that causes the maximum boundary-layer response as the most effective mode. Since boundary-layers on sailplane wings have thickness in the order of a few millimeters, the most effective modes are long streamwise aligned tubes (e.g. low frequency) with diameters in the 10 to 20 millimeter range. Such a tube is hard to imagine, but exists as a Fourier mode of the large-scale turbulent structures.

Holding the most effective ratio  $\delta/\beta$  fixed and varying  $\beta$  produces a curve of the amplitude response versus spanwise length-scale. Figure 4-b compares the computed variation (lines) with data derived from experimental cross-correlation measurements of Kendall. Although the experimental data is inaccurate at low values of  $\beta$  due to the limited span (in  $z$ ) of the measured data, the overall agreement is surprisingly good. The pronounced peak displays a clear preferential spanwise length-scale for the boundary layer response, but as the measurement location is moved closer to the leading edge the peak disappears [2].

Knowing the most amplified length-scales, we can compare streamwise growth rates with experimental measurements under the assumption that the amplitude of the most effective turbulent mode is proportional to the turbulence intensity. The free-stream turbulence intensity is usually characterized by the root-mean-square (in time) of the signal obtained at a single measurement location. This is unfortunate since the signal contains contributions from modes at all frequencies and all scales. To help the com-

parison with the author's model, Dr. J.M. Kendall at the Jet Propulsion Lab in Pasadena, offered to repeat some of his published measurements using band-pass filtering at various frequencies (e.g. 4-8 Hz, 8-12 Hz, 12-16 Hz and 16-20 Hz at a free-stream velocity of 11.5 m/s). This step facilitates the comparison, since in the model the amplitude in the free-stream is set equal to the measured value in the appropriate frequency range. Recently, Leib et al. [19] followed the model steps discussed herein, substituting the series expansion and the PSE equations with matched asymptotic solutions, and substituting an approximate model for anisotropic turbulence in place of the most amplified mode approximation used herein, but arrived at results almost indistinguishable from the theoretical ones shown in figure 5-a, below.

Figure 5-a shows the measured and computed streamwise growth at various frequencies. Note that at low frequencies the growth is almost linear, in similitude to the transient growth displayed by recent "algebraic growth" models of transition [20]. Figure 5-b compares the measured and computed streamwise velocity profiles at two stations. The maximum value of velocity is about 2.5%, and the associated free-stream turbulence level at this frequency is 0.044%, showing that the boundary-layer has amplified the motion in the free-stream turbulence by a factor of 57, as claimed in the introduction.

At high frequencies we have seen that the stimulation of Tollmien-Schlichting (TS) waves by free-stream turbulence is a very weak process. Nevertheless, it is interesting to investigate what happens when a TS wave is superimposed on the low-frequency streaks.

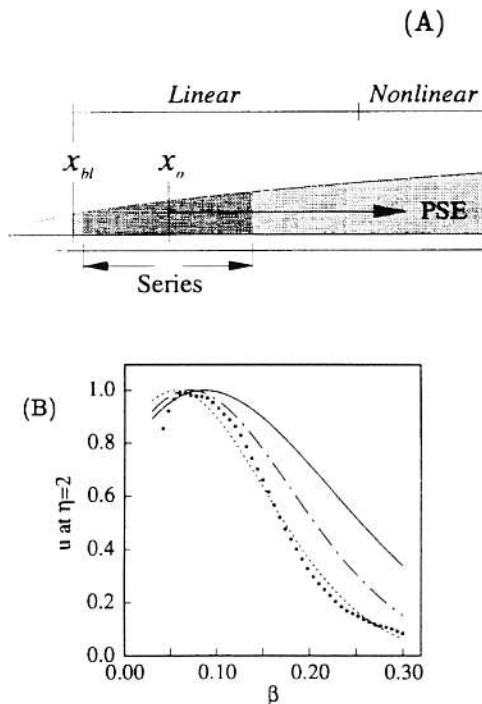


Figure 5: (A) Streak amplitude as function of streamwise distance  $x$  in meters, with nondimensional frequency  $F$  as parameter. Symbols from experiment of Kendall, solid line from model having experimental free-stream turbulence level as input. Free-stream velocity  $U_\infty = 15$  m/s. (B) Comparison with experiment of streamwise velocity profiles at  $x = 178$  and 1118 millimeters  $x$  location, corresponding to  $F = 3$  (solid line) and  $F = 0$  (dashed line). Figures from [2].

For this purpose, we add a TS-wave as given by the Orr-Sommerfeld equation (i.e. we skip the receptivity modeling) to the computed streaks and use the non-linear modeling feature of the PSE to trace the flow-field to the doorsteps of turbulence.

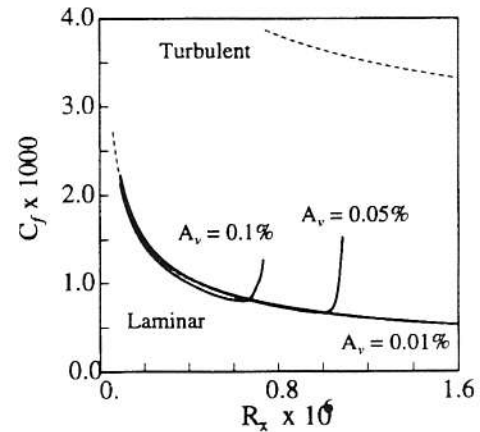


Figure 6: Skin friction versus streamwise position for three levels of the free-stream "B" mode amplitude. The non-linear calculation was started from a pair of streak with  $\beta = 0.06$  and one two dimensional TS wave with frequency  $F = 56$ . Figure from [2].

Figure 6 shows the rise in wall shear stress for three separate runs using different amplitude of the low-frequency atmospheric turbulence component. At the lowest level,  $A_v = 0.01\%$ , the streaks are too weak to trip the flow into turbulence, but increasing the level to  $A_v = 0.05\%$  leads to transition. Lastly, we note that, conceptually, streaks may trigger transition without the presence of a TS wave if the streak's amplitude increases to the point that strong local shear layers form within the streak's velocity field and undergo an inviscid, Rayleigh-type instability.

### 3.3 THE CONTROLLED EXPERIMENT

The comparison with experimental data discussed above is made difficult by the lack of knowledge about the actual state (spatial scales) of the anisotropic turbulence present in the wind-tunnel. Since the "A" and "B" mode expansion can be used to reconstruct any vortical field in the free-stream, Kendall suggested to replace the free-stream turbulence by a single vortex generated at the tip of a small wing oriented perpendicular to the plate's surface and position with a slight angle of attack, so as to generate lift [21]. Figure 7-a shows a schematic of the set-up. The vortex was steady and could be controlled and positioned with precision. The "B" mode expansion was obtained by performing a Fourier-transform of the vortex's velocity field. For each mode, the analysis discussed above was performed, and the total response was obtained by linear superposition. A comparison of the computed and measured streamwise velocity field inside the boundary layer is shown in figure 7-b. The good agreement obtained within this controlled environment gave further validity to the theoretical model<sup>3</sup>.

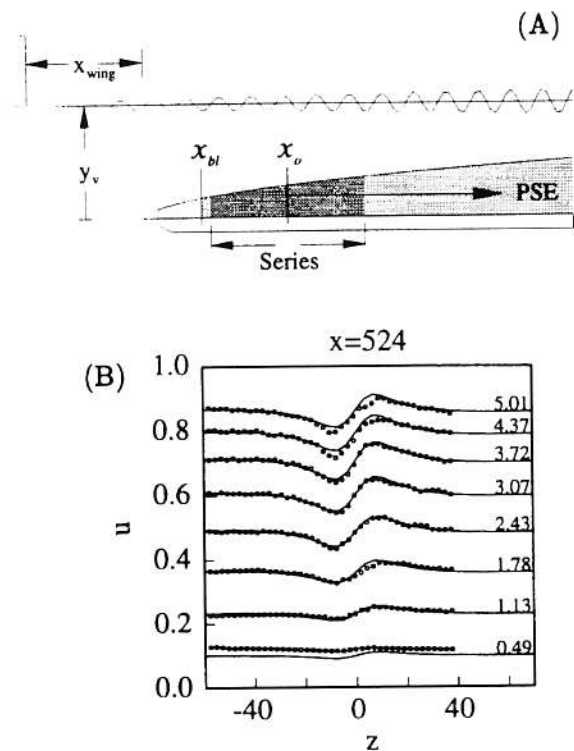


Figure 7: (A) Sketch of the controlled experiment employing a wing-tip generated vortex. (B) Comparison between theory and experiment of the streamwise velocity measured along a spanwise traverse at constant height above the plate. The height is indicated for each traverse shown. The vortex axis is at  $z = 0$  and  $y = 14$ , and the streamwise location of the measurements is  $x = 581$  mm. The free-stream velocity is 3.0 m/s. Figures from [21].

#### 4 CONCLUSION

Experiments and theory on the response of the Blasius boundary layer to free-stream turbulence may shed some light on the loss of glide performance of sailplanes entering the turbulent air flow in a thermal.

Although the atmospheric turbulence contains energy over a large frequency range, including frequencies that match those of unstable Tollmien-Schlichting (TS) waves in the wing's boundary-layer, we provide several reasons why the coupling between atmospheric turbulence and TS waves is in general very weak and, alone, is unlikely to cause transition.

On the other hand, the response of the laminar boundary-layer to the low-frequency components of atmospheric turbulence is very strong, resulting in motions that are orders of magnitude larger than those of the turbulence itself. Some of the main characteristics of these low-frequency motions, known as Klebanoff-modes or streaks, are presented herein, as well as comparisons between experimental measurements and theory. We show that the combination of streaks and a weak TS wave leads to transition, and note that, conceptually, streaks alone can trigger transition upon reaching a sufficiently high amplitude.

#### REFERENCES

[1] KLEBANOFF, P. S., TIDSTROM, K. D. Evolution of amplified waves leading to transition in a boundary-layer with zero pressure gradient. Tech. Note D-195, NASA, 1959.

[2] BERTOLOTTI, F. P. Response of the Blasius boundary layer to free-stream vorticity. *Phys. Fluids A*, 9 (8): 2286-2299, 1997.

[3] KENDALL, J. M. Experimental study of disturbances produced in a pre-transitional laminar boundary layer by weak free stream turbulence. Paper 85-1695, AIAA, 1985.

[4] BRADSHAW, P. The effect of wind-tunnel screens on nominally two-dimensional boundary layers. *J. Fluid Mech.*, 22: 670-687, 1965.

[5] KENDALL, J. M. Boundary-layer receptivity to free stream turbulence. Paper 90-1504, AIAA, 1990.

[6] WESTIN, A. V., BOIKO, B. G. B., KLINGMANN, G. B., KOZLOV, V. V., ALFREDSSON, P. H. Experiments in a boundary layer subjected to free stream turbulence. part 1. boundary layer structure and receptivity. *J. Fluid Mech.*, 281: 193-218, 1994.

[7] KACHANOV, Y. S., KOZLOV, V. V., LEVCHENKO, V. Y. Origin of Tollmien-Schlichting waves in boundary layer under the influence of external disturbances. *Izv. Akad. Nauk. SSSR, Mekh. Zhidk. Gaza*, 5: 85-94, 1977. *Trans: Fluid Dyn.* 1979, 13: 704-11.

[8] NISHIOKA, M., MORKOVIN, M. V. Boundary-layer receptivity to unsteady pressure gradients: experiments and overview. *J. Fluid Mech.*, 171: 219-261, 1986.

[9] GOLDSTEIN, M. E., HULTGREN, L. S. Boundary-layer receptivity to long-wave free-stream disturbances. *Ann. Rev. Fluid Mech.*, 21: 137-166, 1989.

[10] KERSCHEN, E. J. Boundary layer receptivity. Paper 89-1109, AIAA, 1989.

[11] CROUCH, J. D. Theoretical studies on the receptivity of boundary layers. Paper 94-2224, AIAA, 1994.

[12] CHOUDHARI, M., STREET, G. L. Theoretical prediction of boundary-layer receptivity. Paper 94-2223, AIAA, 1994.

[13] HILL, D. C. Adjoint systems and their role in the receptivity problem for boundary layers. *J. Fluid Mech.*, 292: 183-204, 1995.

[14] CROW, S. C. The spanwise perturbation of two-dimensional boundary layers. *J. Fluid Mech.*, 24: 153-164, 1966.

[15] BERTOLOTTI, F. P., HERBERT, TH., SPALART, P. R. Linear and nonlinear stability of the Blasius boundary layer. *J. Fluid Mech.*, 242: 441-474, 1992.

[16] CHU, B. T., KOVASZNYI, L. S. G. Non-linear interactions in a viscous heat-conducting compressible gas. *J. Fluid Mech.*, 3: 494-514, 1958.

[17] BERTOLOTTI, F. P. Transition modelling based on the PSE. In *Transition and Turbulence Modelling*. Kluwer Academic Publishers, June 1995.

[18] HERBERT, TH. Parabolized stability equations. *Ann. Rev. Fluid Mech.*, 29: 245-283, 1997.

[19] LEIB, S. J., WUNDROW, D. W., GOLDSTEIN, M. E. Effect of free-stream turbulence and other vortical disturbances on a laminar boundary layer. *J. Fluid Mech.*, 380: 169-204, 1999.

[20] REDDY, S. C., SCHMID, P. J., BAGGETT, J. S., HENNINGSON, D. S. On the stability of streamwise streaks and transition thresholds in plane channel flows. *J. Fluid Mech.*, 365: 269-303, 1998.

[21] BERTOLOTTI, F. P., KENDALL, J. M. Response of the Blasius boundary layer to controlled free-stream vortices of axial form. Paper 97-2018, AIAA, 1997.